Local galactic kinematics from Hipparcos proper motions

F. Mignard

Observatoire de la Côte d'Azur, CERGA, UMR CNRS 6527, av. Copernic, 06130 Grasse, France

Abstract. The stellar velocity field within two kiloparsecs of the solar system is investigated from the Hipparcos proper motions and parallaxes of about $20\,000$ single stars farther than 100 pc. The motion of the sun relative to the Local Standard of Rest and the relative systematic velocity field due to the galactic rotation are studied simultaneously for several categories of stars ranging from early type dwarfs to K and M giants observed by Hipparcos. The relative velocity field is modeled in the framework of the Milne-Ogorodnikov hydrodynamic representation and led to the determination of eight parameters characterizing the flow, including the usual Oort Constants. The peculiar motion of these stars is also studied from the residuals and led to a new determination of the components of the velocity dispersion for every class of stars considered.

The components of the solar motion are ascertained to within $\pm\, 0.2 - 0.3\ \mathrm{km\,s^{-1}}$ in each direction and are found to vary significantly with the star sample, except for the component normal to the galactic plane always close to $7\ \mathrm{km\,s^{-1}}$. Regarding the Oort constants, one finds $A = 11.0 \pm 1.0\ \mathrm{km\,s^{-1}kpc^{-1}}$ for early type dwarfs and $A = 14.5 \pm 1.0\ \mathrm{km\,s^{-1}kpc^{-1}}$ for the distant giants. The constant B shows a less obvious difference with respectively $-13.2 \pm 0.5\ \mathrm{km\,s^{-1}kpc^{-1}}$ and $-11.5 \pm 1.0\ \mathrm{km\,s^{-1}kpc^{-1}}$. The galactic center is found to lag by 6 degrees from the normal to the direction of the galactic motion of the LSR in the solar neighborhood. Finally the three components of the velocity dispersion are determined and discussed for all the stellar groups considered in this paper with an accuracy of $\pm\, 0.2 - 0.4\ \mathrm{km\,s^{-1}}$.

Key words: astrometry – celestial mechanics, stellar dynamics – Galaxy: kinematics and dynamics – Galaxy: solar neighbourhood

1. Introduction

Local stellar kinematics is the study of the motion of the stars in the solar neighborhood to distances of few kiloparsecs. The motion of these stars is governed by the gravitational potential of all the stars in the Galaxy and depends on the mass distribution. To a large extent the set of stars comprising the solar

---

Send offprint requests to: F. Mignard (mignard@obs-azur.fr)

neighborhood behaves like a collisionless gas implying that the gravitational potential is a smooth function of position. Associated to the star counts, stellar kinematics is also a powerful method for probing the structure and the evolution of the Milky Way.

The determination of the size and structure of the Milky Way was one of the highlights of the nineteenth century astronomical research which culminated dramatically with the Great Debate in 1920 and the ensuing epoch-making discoveries of E. P. Hubble (Hoskin, 1982, North, 1990). The modern investigations on the observational effect of the Galactic rotation started with the works of Lindblad (1925) and Oort (1927a, 1927b) who developed the model of the axial rotation with the rate depending only on the distance to the galactic center. The simple hypothesis of differential axisymmetric rotation was sufficient to account for the systematic stellar motion (the double sine-wave) with the Galactic longitude. Oort, 1927a, introduced the two constants A and B and derived the simple formulae for describing the observable consequences of the Galactic rotation. Using the proper motions together with the radial velocities in his second paper (Oort, 1927b) he found $A = 19\ \mathrm{km\,s^{-1}kpc^{-1}}$ and $B = -24\ \mathrm{km\,s^{-1}kpc^{-1}}$.

The average motion of a set of stars at any point the Galaxy can be modeled as a stream, the kinematics of which is that of the overall galactic rotation. The kinematics of the individual stars is then defined as the superimposition of the net flow of the LSR, a possible streaming motion of the population of these stars and by the individual scatter with respect to the mean motion. Thus the local kinematics of the Milky Way can be conveniently divided into three different, but connected, problems:

1. The motion of the Sun relative to the average motion of stellar groups in the solar neighborhood,
2. The differential velocity field due to the galactic rotation (shear motion) around the Sun considered as the remaining systematic motion when the individual and small scale stellar motions are removed,
3. The peculiar velocities of the stars relative to the rotating flow for the various stellar groups and due to the repeated interactions of each star with the neighboring ones or with large molecular clouds.

The basic observational material from which the above kinematics properties of the various stellar populations have been studied is the radial velocity v_R and the tangential proper motion μ_T relative to the Sun and scores of works have appeared in the intervening years. Closely related to the present work, both in methodology and objectives, is the paper by Miyamoto & Sôma, 1993a in which the authors investigate the systematic stellar velocity field of a set of K and M giants in order to determine the possible lack of inertiality of the FK5 system and consequently that of the proper motion system.

For years discussions about the rotational parameters of the local velocity field of the stars in the solar neighborhood have been hampered by the difficulty to realize a good decoupling with the fact that the components of the proper motions were referred to a rotating frame. The arrival of astrometric measurements from space provides a new boost in stellar kinematics and the availability of the Hipparcos Catalogue with its high quality and homogeneous proper motions referred to a non rotating frame, was the main motivation behind this work. In a paper published just after the launch of Hipparcos, Ratnatunga, 1992 stated that with this new technique *we are truly at the dawn of a new era in the study of galactic structure by stellar kinematics.*

Although the Hipparcos data is incomplete, since no radial velocity is available at the moment in a comprehensive way, the proper motion components and the distance are available for all the program stars, providing at the same time the angular displacement with the proper motion and the tangential velocity with

$$v_T = 4.7405 \, \frac{\mu_T}{\pi} \tag{1}$$

where the proper motion is expressed in mas/year, the parallax in mas and the velocity in km s^{-1}. It was then tempting to take advantage of these properties to study, in a single adjustment on an unbiased sample with many stars belonging to virtually all spectral classes, the various components of the stellar motion.

This is the main goal of this paper which is organized into three main parts:

– The presentation of the formalism which relates the diverse sources of the stellar motion to the observable quantities,
– A discussion on the selection of observing material and the binning of stars into homogeneous categories,
– The presentation and discussion of the results on the solar motion, the local galactic shear motion and the peculiar velocities of the stars as a function of the spectral type and luminosity class.

The paper does not bring fundamentally new results in this area but, hopefully, put in a much firmer basis, (thanks to the number of stars, the high quality proper motions, the non-rotating frame and the homogeneity of the samples), results that have appeared over the years on either of the three components of the stellar kinematics within ≈ 2 kpc of the Sun.

2. The observing material

The recently published Hipparcos Catalogue provides astronomers with the best optical materialisation of the International Reference System (ICRS) defined and realized by a set of radio sources observed in VLBI.

The primary result is an astrometric catalogue of 118 218 entries nearly evenly distributed over the sky with an astrometric precision in position, proper motion and parallax of 1 mas or mas/yr, or better for the brightest stars. The optical reference frame defined by the Hipparcos positions and proper motions is believed to have a global accuracy of about 0.1 mas and 0.1 mas/yr with no regional distortion. The median magnitude of the Catalogue is $Hp = 8.7$ and half of the Catalogue lies in the interval $8 < Hp < 9.5$. A more comprehensive presentation of the astrometric properties of the Catalogue is available in Perryman et al., 1997, Mignard, 1997 and in the documentation published with the Hipparcos Catalogue (ESA, 1997).

Regarding the present work there are four main aspects of the Catalogue particularly relevant:

– The reference frame to which the positions and proper motions are referred,
– The parallaxes and their validity for the most distant stars,
– The accuracy and precision of the proper motions
– The completeness of the catalogue for each class of brightness.

The Catalogue has been initially constructed in a frame with a non-zero rotation with respect to the inertial frame. Then it was linked to the extragalactic frame with various methods involving objects common to Hipparcos and to VLBI or proper motion programs tied to the extragalactic frame (Kovalevsky & Lindegren, 1995, Kovalevsky et al., 1997). By construction, the Hipparcos reference frame is an extension of the FK5(J2000) frame, but independent of any assumption about the precession constant or about the non precessional motion of the equinox, a fact of the utmost importance for interpreting the rotational terms and the Oort constant B. One can thus state that the Hipparcos positions and proper motions provide a realisation of an optical non-rotating reference frame with axes pointing to fixed extragalactic directions. The accuracy of the link corresponds to a standard error of 0.6 mas in the alignment of the axes at the Catalogue epoch J1991.25 and 0.25 mas yr^{-1} in the rate of rotation, meaning that the Hipparcos proper motion system is quasi inertial to within ± 0.25 mas yr^{-1}. One must stress in the context of this paper that this uncertainty translates into a systematic effect of similar magnitude in the Hipparcos system of proper motions with respect to an inertial frame, and not into a random error which would average out over a large data set. This uncertainty becomes 1.2 $\text{km s}^{-1}\text{kpc}^{-1}$ on the rotational components of the velocity field and similarly on the Oort B constant..

The consistency of the Hipparcos induced reference frame is better than its link to the extragalactic frame. The proper motions of the Hipparcos Catalogue define a consistent reference frame (albeit rotating) which is likely to be accurate on a global scale
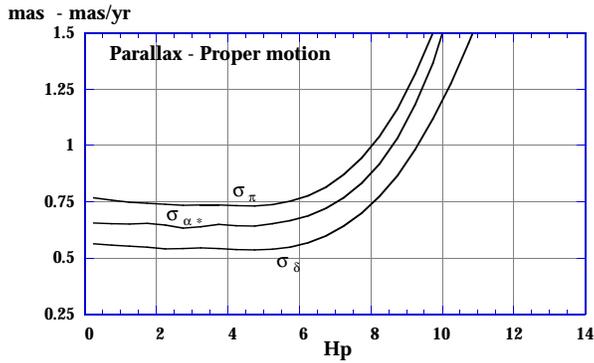
Fig. 1. Medians of the standard errors at J1991.25 of the parallax and proper motions in the Hipparcos Catalogue as a function of the Hipparcos magnitude. The standard errors are expressed in mas for the parallax and in mas/yr for the components of the proper motion. Only the $\sim 100\,000$ single stars of the Catalogue are considered in this plot.

Fig. 2. The global galactic coordinate system CX, CY, CZ and the local galactic coordinate system centered at the LSR used in this paper. C is the centre of the Galaxy and S the solar LSR.

to at least $0.1\ \mathrm{mas\,yr^{-1}}$, and maybe ten times better due to the large number of stars, although there is no means to assess that more precisely with current techniques. Ultimately the research presented in this paper has been motivated by the quality of the proper motions and the quasi-inertiality of the reference frame together with its independence from the precession constant.

The Hipparcos parallaxes are trigonometric and by construction virtually absolute, in the sense that they do not use reference background stars. Numerous analyses of the Hipparcos parallaxes with the preliminary and final solutions confirm this view and indicate that the global zero-point offset, common to all stars, is smaller than 0.1 mas (Arenou et al., 1995; ESA, 1997). A recent search of a global zero–point in the parallaxes in the 5.4×10^6 residuals of the astrometric data by **?** supports also this claim with a non significant offset of -0.010 ± 0.010 mas. Most of the statistical analysis of this paper rests on the basic assumption that, while the individual parallaxes of stars farther away than 1 kpc are not reliable individually whenever $\sigma_\pi/\pi > \sim 1$, the full set of Hipparcos parallaxes constitutes an homogeneous and unbiased sample down to $\pi \approx 0.1 - 0.2$ mas. For the most distant stars it is likely that spectroscopic parallaxes are sometimes better and should have been preferred. However, it is hard to devise a sensible way to decide which stars to handpick without introducing systematic differences with the Hipparcos sample. As a consequence, in this work we stick to the Hipparcos data, favoring the statistical homogeneity to any other criterion, even though this might be done at the cost of the accuracy of few parallaxes.

The same argument is valid for the radial velocity not yet available for all Hipparcos stars, but which exists for several thousands of them and could have been used to increase the number of observation equations, with the risk of obscuring the interpretation of the results. In addition the systematic velocity field induced by the Galactic rotation is independent of the distance of the stars when assessed through the proper motion components, while it is directly proportional to the stellar distance for the radial velocity. As pointed out by Crézé, 1970 the
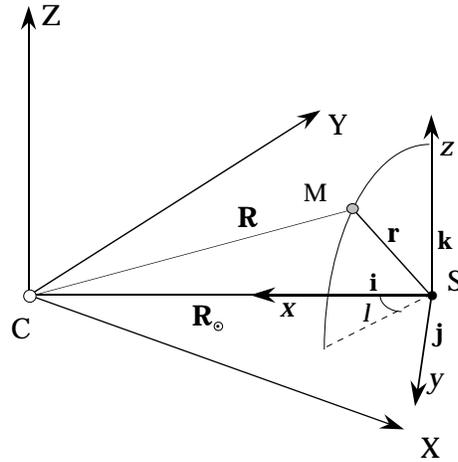
asymmetry in the distribution of errors in the distances causes the value of the Oort constant A to be underestimated. The analysis with proper motion does not suffer from such a drawback.

The precision of the proper motions and of the parallaxes is shown in Fig. 1 as a function of the magnitude. Knowing that the bulk of the Hipparcos Catalogue is between magnitudes 7.5 to 9.5, this shows that most of the parallaxes used in this paper are in the range of the mas accuracy and that the proper motion components are slightly better than 1 mas/yr.

3. The differential velocity field

3.1. Reference frames

Let C be the center of the Galaxy. We define the three orthogonal directions with the origin in the solar neighborhood and the unit vectors $\mathbf{i}$, $\mathbf{j}$, $\mathbf{k}$ pointing respectively to the galactic center, positive in the direction of the galactic rotation and normal to the galactic plane in the direction of the north galactic pole. The corresponding axes are labeled Sx, Sy, Sz. This frame is right-handed.

One must be very careful in choosing reference frames to express the observation equations because of the possible inconsistencies between the mathematical needs, based on right-handed orthonormal natural frames with the radial direction directed outward from the galactic center ($-\mathbf{i}$ in Fig. 2), and the usual definition of the galactic coordinates, involving the positive x-axis directed toward the center of the Galaxy. The second axis of the natural frame is opposite to the direction of the motion of the Sun, that is to say as $-\mathbf{j}$ in Fig. 2. The tensorial equations are expressed in the natural frame tied to the polar coordinates (see Fig. 4) while the angular coordinates of the stars are transformed from the equatorial coordinates α, δ, $\mu_\alpha \cos\delta$, μ_δ into the standard galactic coordinates l, b, $\mu_l \cos b$, μ_b oriented as shown in Fig. 3. In due course the signs of the equations will be changed accordingly to express the equations in the usual right-handed galactic frame centered at the Sun.
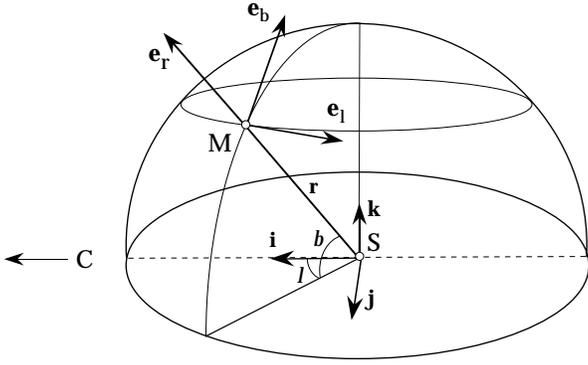
Fig. 3. The galactic coordinate system triad **i**, **j**, **k** and the local triad **e**$_r$, **e**$_l$, **e**$_b$ attached to the spherical coordinates l, b.

Fig. 4. Comparison of the astronomical galactic reference system **i**, **j**, **k**, the local frame associated to the cylindrical coordinates **e**$_r$, **e**$_\theta$, **e**$_z$, and their link with the components of the systematic velocity field of the Galaxy.

3.2. Systematic and peculiar velocities

The velocity vector $\overline{\mathbf{V}}_*$ of each star with respect to the galactic center may be viewed as the sum of two contributions:

- The velocity of the global flow of the galactic material in the vicinity of this particular star. This component will be referred to as the centroid velocity and noted $\mathbf{V} = \mathbf{V}(\mathbf{R}) = \mathbf{V}(X, Y, Z)$. The centroid velocity is a continuous and slowly variable function of the position and is akin to the velocity of a fluid element in a continuous medium.
- The peculiar velocity of that star, (referred to also as the residual velocity) with respect to the centroid and noted $\mathbf{v}_*$. This velocity is connected to the intrinsic motion of the individual stars, whose orbits may be very complex without direct relation to the galactic motion as a whole.

So for any star one has $\overline{\mathbf{V}}_* = \mathbf{V}(\mathbf{R}) + \mathbf{v}_*$, which expresses that the velocity vector relative to the galactic center is the sum of the velocity of the centroid and of the peculiar velocity. The same decomposition holds for the Sun with $\overline{\mathbf{V}}_\odot = \mathbf{V}(\mathbf{R}_\odot) + \mathbf{v}_\odot$. Thus the relative motion of a star with respect to the Sun can be written,

$$\tilde{\mathbf{v}}_* = \overline{\mathbf{V}}_* - \overline{\mathbf{V}}_\odot = [\mathbf{V}(\mathbf{R}) - \mathbf{V}(\mathbf{R}_\odot)] + [\mathbf{v}_* - \mathbf{v}_\odot] \tag{2}$$

where the first bracket stands for the relative velocity fields of the centroids and the second gives the difference between the peculiar velocity of a star and the Sun. The peculiar velocity of the Sun $\mathbf{v}_\odot$ in Eq. (2) is usually referred to as the solar motion toward the solar apex. From its definition it is obvious that it depends on the group of stars selected to define the centroid of the observer.

3.3. The relative velocity field

We derive in this section the basic equations describing the systematic velocity field relative to the Sun due to the Galactic rotation, without any assumption as to the nature of this rotation, apart that it can be represented by a continuous smooth flow. The derivation follows the principles laid out by Ogorodnikov, 1932 and Milne, 1936 (see also Ogorodnikov, 1965) and applied later in similar studies for example by Clube, 1972 with the proper
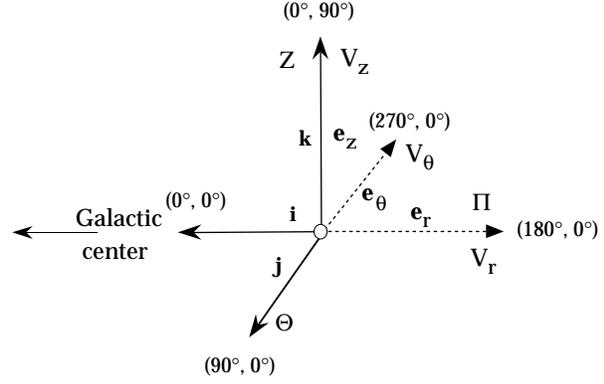
motions of the FK5 or Fricke & Tsioumis, 1975 with the same material limited to the most distant stars. The method has the great advantage of being independent of any a priori dynamical model of the Galaxy, but the defect of being restricted to a local description. Strictly speaking the knowledge of the tensor describing the local change of the velocity field, says nothing about the overall kinematics of the Galaxy, although it provides important constraints on acceptable models.

Let S and M be the centroids associated to the Sun and the star at radius vectors $\mathbf{R}_\odot$ and $\mathbf{R}_*$, and $\mathbf{r} = \mathbf{R}_* - \mathbf{R}_\odot$. To the first order in r/R we have

$$\mathbf{v}(\mathbf{r}) = \mathbf{V}(M) - \mathbf{V}(S) \approx (\mathbf{r} \cdot \nabla)\mathbf{V} \tag{3}$$

which gives for the cartesian components of the relative field, with the implicit summation rule,

$$v_k = T_{kl}\, x^l = \frac{\partial V^k}{\partial X^l}\, x^l \tag{4}$$

where T_{kl}, $k, l = 1, 2, 3$ may be called the velocity strain tensor, by analogy with the strain in the deformation of a continuous medium. With matrix notation Eq. (3) can be written as,

$$\mathbf{v}(\mathbf{r}) = [\mathbf{T}]\mathbf{r} \tag{5}$$

It is convenient to separate $\mathbf{T}$ into its symmetric and antisymmetric parts, $\mathbf{T} = \mathbf{S} + \mathbf{A}$ with

$$S_{kl} = \frac{1}{2}(T_{kl} + T_{lk}), \qquad A_{kl} = \frac{1}{2}(T_{kl} - T_{lk}) \tag{6}$$

As well known, the effect of an antisymmetric application in the usual three dimensional space amounts to a global rotation ω with,

$$[\mathbf{A}]\,\mathbf{r} = \begin{bmatrix} 0 & -\omega_z & \omega_y \\ \omega_z & 0 & -\omega_x \\ -\omega_y & \omega_x & 0 \end{bmatrix} \begin{bmatrix} x \\ y \\ z \end{bmatrix} = \boldsymbol{\omega} \times \mathbf{r} \tag{7}$$

with

$$\omega_x = -A_{yz},\; \omega_y = A_{xz},\; \omega_z = -A_{xy}$$

The components of $\boldsymbol{S}$ and $\boldsymbol{A}$ can be expressed in any curvilinear system by replacing the partial derivatives in Eq. (4) by the co-variant derivatives. In the case of polar coordinates r, θ, z one finds (see for example Love, 1944, Landau & Lifchitz, 1967, Miyamoto & Sôma, 1993a) for the symmetric part,

$$\left.\begin{aligned}
S_{rr} &= \frac{\partial V_r}{\partial r} \\[4pt]
S_{\theta\theta} &= \frac{1}{r}\frac{\partial V_\theta}{\partial \theta} + \frac{V_r}{r} \\[4pt]
S_{zz} &= \frac{\partial V_z}{\partial z} \\[4pt]
2S_{r\theta} &= \frac{\partial V_\theta}{\partial r} - \frac{V_\theta}{r} + \frac{1}{r}\frac{\partial V_r}{\partial \theta} \\[4pt]
2S_{rz} &= \frac{\partial V_r}{\partial z} + \frac{\partial V_z}{\partial r} \\[4pt]
2S_{\theta z} &= \frac{1}{r}\frac{\partial V_z}{\partial \theta} + \frac{\partial V_\theta}{\partial z}
\end{aligned}\right\} \quad (8)$$

and for the antisymmetric part,

$$\left.\begin{aligned}
2\omega_r &= -2A_{\theta z} = \frac{1}{r}\frac{\partial V_z}{\partial \theta} - \frac{\partial V_\theta}{\partial z} \\[4pt]
2\omega_\theta &= 2A_{rz} = \frac{\partial V_r}{\partial z} - \frac{\partial V_z}{\partial r} \\[4pt]
2\omega_z &= -2A_{r\theta} = \frac{\partial V_\theta}{\partial r} + \frac{V_\theta}{r} - \frac{1}{r}\frac{\partial V_r}{\partial \theta}
\end{aligned}\right\} \quad (9)$$

where V_r, V_θ, V_z denote the components of the systematic velocity field $\boldsymbol{V}(\boldsymbol{R})$.

Remarks:

- The components V_r, V_θ, V_z are the coordinates of $\boldsymbol{V}(\boldsymbol{R})$ on the local directions $\mathbf{e}_r$, $\mathbf{e}_\theta$, $\mathbf{e}_z$ as shown in Fig. 4 with θ oriented counter-clockwise. Therefore one has $\Theta = -V_\theta$. The linear expansion $[\mathbf{S}]\,\boldsymbol{r} + [\mathbf{A}]\,\boldsymbol{r}$ gives the components of the velocity field relative to the LSR on the same triad, provided that $\boldsymbol{r}$ is also projected on the same basis.
- The components S_{kl} of $\mathbf{S}$ and ω_k of $\boldsymbol{\omega}$ are also given on the same triad. To express the tensor $\mathbf{S}$ on the triad $\mathbf{i}$, $\mathbf{j}$, $\mathbf{k}$ of the galactic coordinates one must change the sign of S_{rz}, $S_{\theta z}$, ω_r, ω_θ, independently of the signs of the derivatives when needed. For example, the term ω_z should be identified to the Oort constant B representing the vorticity of the field and classically given in a model with circular motion by

$$B = -\frac{1}{2}\left[\frac{\Theta}{R_0} + \frac{d\Theta}{dR}\right]$$

is the same as ω_z once the signs are changed. The constant B is negative and so is ω_z since $V_\theta = -\Theta$ is negative. A similar remark holds true for $S_{r\theta}$ to be identified with the Oort constant A modelling the shear deformation as,

$$A = \frac{1}{2}\left[\frac{\Theta}{R_0} - \frac{d\Theta}{dR}\right]$$

which is positive while V_θ/r in Eq. (8) is negative.

It is easy from Eqs. (8) to write down the cartesian components of the relative velocity on the triad $\mathbf{i}$, $\mathbf{j}$, $\mathbf{k}$, with $\boldsymbol{r} = (x, y, z) = (r\cos l\cos b,\ r\sin l\cos b,\ r\sin b)$, by changing $S_{rz} \to -S_{rz}$ and $S_{\theta z} \to -S_{\theta z}$, to express the tensors on this triad, keeping in mind that the right-hand sides of Eqs. (8)-(9) are left unchanged,

$$\left.\begin{aligned}
v_x &= S_{rr}\,r\cos l\cos b + S_{r\theta}\,r\sin l\cos b - S_{rz}\,r\sin b \\
v_y &= S_{r\theta}\,r\cos l\cos b + S_{\theta\theta}\,r\sin l\cos b - S_{\theta z}\,r\sin b \\
v_z &= -S_{rz}\,r\cos l\cos b - S_{\theta z}\,r\sin l\cos b + S_{zz}\,r\sin b
\end{aligned}\right\} \quad (10)$$

This must be now expressed on the local triad $\mathbf{e}_r$, $\mathbf{e}_l$, $\mathbf{e}_b$ attached to the spherical coordinates l, b of the star at M by,

$$\left.\begin{aligned}
v_r &= v_x\cos b\cos l + v_y\cos b\sin l + v_z\sin b \\
v_l &= -v_x\sin l + v_y\cos l \\
v_b &= -v_x\sin b\cos l - v_y\sin b\sin l + v_z\cos b
\end{aligned}\right\} \quad (11)$$

By inserting 10 in 11 one gets the relationship between the components of the proper motion and the components of the velocity gradient as,

$$\begin{aligned}
V_r/r =\ & S_{rr}\,\cos^2 l\cos^2 b + S_{\theta\theta}\,\sin^2 l\cos^2 b \\
& + S_{zz}\,\sin^2 b + S_{r\theta}\,\sin 2l\cos^2 b \\
& - S_{rz}\,\cos l\sin 2b - S_{\theta z}\,\sin l\sin 2b
\end{aligned} \quad (12)$$

$$\begin{aligned}
\mu_l\cos b =\ & -\frac{S_{rr}}{2}\sin 2l\cos b + \frac{S_{\theta\theta}}{2}\sin 2l\cos b \\
& + S_{r\theta}\,\cos 2l\cos b + S_{rz}\,\sin l\sin b \\
& - S_{\theta z}\,\cos l\sin b
\end{aligned} \quad (13)$$

$$\begin{aligned}
\mu_b =\ & -\frac{S_{rr}}{2}\cos^2 l\sin 2b - \frac{S_{\theta\theta}}{2}\sin^2 l\sin 2b \\
& + \frac{S_{zz}}{2}\sin 2b - \frac{S_{r\theta}}{2}\sin 2l\sin 2b \\
& - S_{rz}\,\cos l\cos 2b - S_{\theta z}\,\sin l\cos 2b
\end{aligned} \quad (14)$$

A similar procedure applied to the antisymmetric part of the velocity field gives the components of the rotational field expressed with the components of ω as,

$$\left.\begin{aligned}
v_x &= -\omega_z\,r\sin l\cos b - \omega_\theta\,r\sin b \\
v_y &= \omega_z\,r\cos l\cos b + \omega_r\,r\sin b \\
v_z &= \omega_\theta\,r\cos l\cos b - \omega_r\,r\sin l\cos b
\end{aligned}\right\} \quad (15)$$

which leads to with Eq. 11,

$$v_r = 0 \quad (16)$$

$$\mu_l\cos b = \omega_z\,\cos b + \omega_\theta\,\sin l\sin b + \omega_r\,\cos l\sin b \quad (17)$$

$$\mu_b = \omega_\theta\,\cos l - \omega_r\,\sin l \quad (18)$$

As said earlier with, $S_{r\theta}$ being the same as the Oort constant A and ω_z as B, the usual dependence in galactic longitude and latitude is recovered in Eqs. (13)-(14) and in Eq. (17).

3.4. Combinations of related terms

We introduce now several combinations of the unknowns S_{kl} and ω_i which have a more direct physical interpretation in term of amplitudes and phases.

3.4.1. Combination of $S_{r\theta}$, S_{rr}, $S_{\theta\theta}$, S_{zz}

By selecting in Eqs. (13)-(14) the relevant terms one has,

$$\mu_l \cos b = \cos b \left[S_{r\theta} \cos 2l - (\frac{S_{rr}}{2} - \frac{S_{\theta\theta}}{2}) \sin 2l \right] \quad (19)$$

$$\mu_b = -\frac{\sin 2b}{2} \left[S_{r\theta} \sin 2l + (\frac{S_{rr}}{2} - \frac{S_{\theta\theta}}{2}) \cos 2l \right]$$
$$\quad - \frac{\sin 2b}{2} \left[\frac{S_{rr}}{2} + \frac{S_{\theta\theta}}{2} - S_{zz} \right] \quad (20)$$

which leads to the introduction of the generalized Oort constants A, C, K or $\bar{A}$, ϕ, K with an obvious identification of terms, not detailed in this derivation,

$$\mu_l \cos b = A \cos 2l \cos b - C \sin 2l \cos b$$
$$= \bar{A} \cos b \cos(2l - 2\phi) \quad (21)$$

$$\mu_b = -\frac{A}{2} \sin 2l \sin 2b - \frac{C}{2} \cos 2l \sin 2b - \frac{K}{2} \sin 2b$$
$$= -\sin b \cos b \left[\bar{A} \sin(2l - 2\phi) + K \right] \quad (22)$$

One sees from Eqs. (19)-(20) that only the combinations $S_{rr} - S_{zz}$ and $S_{\theta\theta} - S_{zz}$ can be determined with the components of the proper motion.

3.4.2. Combination of S_{rz}, $S_{\theta z}$

Again from Eqs. (13)-(14),

$$\mu_l \cos b = -S_{rz} \sin l \sin b + S_{\theta z} \cos l \sin b$$
$$= A' \sin b \sin(l - \psi) \quad (23)$$

$$\mu_b = S_{rz} \cos l \cos 2b + S_{\theta z} \sin l \cos 2b$$
$$= A' \cos 2b \sin(l - \psi) \quad (24)$$

3.4.3. Combination of ω_r, ω_θ, ω_z

Directly from Eqs. (17) - (18) one writes,

$$\mu_l \cos b = -\sin b[\omega_r \cos l + \omega_\theta \sin l] + \omega_z \cos b$$
$$= -B' \sin b \cos(l - \chi) + B \cos b \quad (25)$$

$$\mu_b = \omega_r \sin l - \omega_\theta \cos l$$
$$= -B' \sin(l - \chi) \quad (26)$$

where B is the Oort Constant linked to the rotational deformation of the local velocity field while B' and χ are related to a possible global in-plane rotation.

3.5. Final formulae with the physical parameters

For the sake of completeness the final equations for the systematic velocity field in the solar neighborhood are collected below, including the radial velocity not used with the proper motion data,

$$\mu_l \cos b = \bar{A} \cos b \cos(2l - 2\phi) + A' \sin b \cos(l - \psi)$$
$$+ B \cos b - B' \sin b \cos(l - \chi) \quad (27)$$

$$\mu_b = -\frac{\bar{A}}{2} \sin 2b \sin(2l - 2\phi) + A' \cos 2b \sin(l - \psi)$$
$$- \frac{K}{2} \sin 2b + B' \sin(l - \chi) \quad (28)$$

$$v_r = \bar{A} \cos^2 b \sin 2(l - 2\phi) + A' \sin 2b \sin(l - \psi)$$
$$+ K \cos^2 b + Z \quad (29)$$

Remarks:

– If the proper motions are expressed in mas/yr, the generalized Oort constants in $\text{km s}^{-1}\text{kpc}^{-1}$ and V_r in km s^{-1}, the right–hand side of the equations for the proper motion must be divided by $k = 4.7405$ (Eq. (1)). This remark applies to the next section too.

– The non-linear equations taken in the form 27-29 are convenient for discussions. However the least squares fit will be performed on their linear equivalents with the S_{kl} as unknowns.

4. The peculiar solar velocity

We consider the rectangular system of galactic coordinates **i**, **j**, **k** with the origin at the observer. If $\boldsymbol{v}_\odot = (u_\odot, v_\odot, w_\odot)$ are the components of the solar motion with respect to the LSR on this triad, the effect on the proper motion of the stars is given by the reflex motion $-\boldsymbol{v}_\odot$ and yields by direct application of Eqs. (11),

$$V_r = -u_\odot \cos l \cos b - v_\odot \sin l \cos b - w_\odot \sin b \quad (30)$$
$$\mu_l \cos b = \pi(u_\odot \sin l - v_\odot \cos l) \quad (31)$$
$$\mu_b = \pi(u_\odot \cos l \sin b + v_\odot \sin l \sin b - w_\odot \cos b) \quad (32)$$

where π is the parallax of the star.

5. Observation equations

The model to be fitted to the observed proper motions comprises Eqs. (13), (17) and (31) for the proper motion in galactic longitude and Eqs. (14), (18) and (32) for the proper motion in galactic latitude. This can be written formally as,

$$\mu_l \cos b = \Phi(S_{kl}, \omega_k, u_\odot, v_\odot, w_\odot) + \epsilon_l \quad (33)$$
$$\mu_b = \Psi(S_{kl}, \omega_k, u_\odot, v_\odot, w_\odot) + \epsilon_b \quad (34)$$

where S_{kl} stands for $S_{rr}, \cdots$ and ω_k for $\omega_r, \omega_\theta, \omega_z$. The random terms ϵ_l and ϵ_b in Eq. (33)-(34) include the true random errors of the observed proper motion components and the contribution of the peculiar velocity of each star. The Hipparcos positions and proper motions given in equatorial coordinates are transformed in galactic coordinates and the full covariance matrix is evaluated in the same system by using the ten correlation coefficients available in the Hipparcos Catalogue. All the subsequent computations are performed in galactic coordinates.

5.1. Selection of the stars

The present work rests mainly on the statistical combination of many stars sufficiently well distributed over galactic longitudes
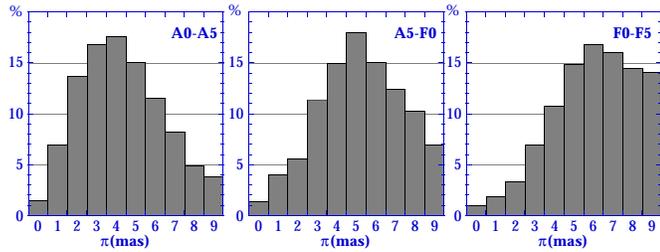
Fig. 5. Parallax distribution for the early type dwarf stars meeting the selection criteria of this paper. The galactic differential motion is visible on the most distant stars whereas the motion of the nearby stars is sensitive to the peculiar motion of the Sun.
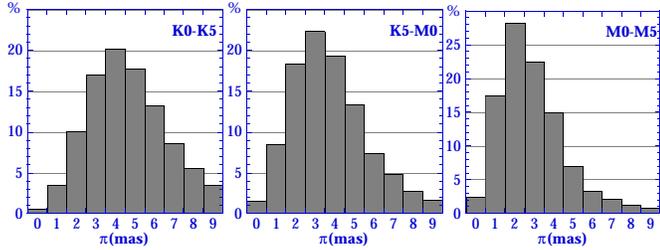
Fig. 6. Same as Fig. 5 for the late type giants.

and latitudes, spectral classes and types. Each category retained for the analysis must be as homogeneous as possible to avoid risking to invalidate the conclusions. It is also highly desirable to avoid any a priori statistical bias in the selection resulting from the content of the Hipparcos Catalogue. This has led to a stringent selection of objects from the following criteria.

1. Only the single stars have been retained on the basis that their astrometric solution is on the average of better quality than that of the double and multiple stars. Furthermore, the selection according to the spectral type or color index becomes rather meaningless for a multiple systems.

2. The second criterion deals with the selection of stars lying in a certain range of distances. The effect of the solar motion is in principle stronger on stars in the immediate vicinity of the Sun, since the reflex proper motion decreases linearly with the parallax. On the other hand the systematic motion due to the galactic rotation reveals itself essentially on stars farther than ≈ 500 pc, since a Oort constant of the order of $10 \text{ km s}^{-1}\text{kpc}^{-1}$ gives rise to an angular displacement of 2 mas/yr at 1 kpc. But the peculiar velocities of the stars being typically of 20 km s^{-1}, this produces a significant noise in the data for stars closer than ≈ 100 pc. After several trials followed by a statistical analysis of the residuals, only stars with $0.5 < \pi < 10$ mas were retained, that is to say for distances in the range 0.1 to 2 kpc. One must add that for the smaller parallaxes this selection has only a statistical meaning, since the typical uncertainty of each parallax is about 1 mas. Many stars with Hipparcos parallaxes between 0.5 and 1 mas might be much farther than indicated or as close as few hundred parsecs. However on the average the selection corresponds to the limits quoted without bias.
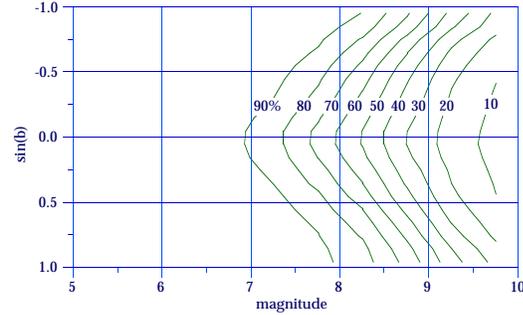
Fig. 7. *Contour lines for the level of completeness of the Hipparcos Catalogue as a function of the V magnitude and of the galactic latitude. Lines are labelled in percentage of completeness.*

3. One major risk is to create statistical bias just because of the content of the Hipparcos Catalogue in which the survey is limited to the brightest stars, which on the average are also the less distant. To limit this risk, the completeness of the Hipparcos Catalogue has been investigated as a function of the galactic latitude, magnitude and colors in a much more detailed way than from the limited information provided by the survey flag of the Catalogue. The Tycho Catalogue is known to be roughly ninety percent complete at $V = 10.5$ and virtually complete for stars brighter than 9 mag (ESA, 1997). In the average the completeness of Hipparcos is limited to stars brighter than 7 - 7.5 mag, thus well within the overall completeness of Tycho. It was then possible to make a detailed map of the Hipparcos completeness in the different regions of the sky and as a function of the magnitude and color, just by comparing to Tycho, at least up to $V = 10.5$. The overall dependence in galactic latitude and magnitude, irrespective of color is shown in Fig. 7. In this diagram the main feature reflects the definition of the survey in the Hipparcos programme. Then for the analysis discussed in this paper, only stars belonging to a bin of magnitude, color and galactic latitude with a completeness larger than 70 percent in the Hipparcos Catalogue have been selected as suitable. At low galactic latitude this corresponds to a limit magnitude of 7.7, while fainter stars are progressively selected at higher galactic latitude. These boundaries are slightly variable with the star colors, typically half magnitude fainter for early type stars and half magnitude brighter for the red stars. This procedure, while leaving out many useful stars, is a safety net against selection biases that could have been incriminated just from the content of the Catalogue.

4. The stars in the solar neighborhood can be distributed into many groups in terms of their velocities, or more precisely according to the velocity dispersion found within each group. In the disk population this is intimately connected to the spectral type: young and early type stars are less dispersed than late type dwarfs or giants. This implies that the typical ϵ_l and ϵ_b in Eqs. (33)-(34) change significantly with the category of stars. This leads naturally to divide the available sample of stars into small groups rather homogeneous

Table 1. Data used in this paper

$B - V$	Spect. type	No. stars	% $|b| < 30$	V_{scat} km/s	V_{max} km/s
[0.00, 0.15]	A0 - A5	3936	74	12.5	62
[0.15, 0.30]	A5 - F0	3163	57	15.0	70
[0.30, 0.45]	F0 - F5	3098	37	17.1	75
[0.85, 1.15]	K0 - K5	6246	35	21.0	88
[1.15, 1.40]	K5 - M0	3459	37	21.0	88
[1.40, 1.60]	M0 - M5	2492	42	21.0	88

in term of stellar evolution, and to solve the observations equations independently one group at a time.

5. This selection is not yet sufficient to ensure that all the stars of a given spectral type and luminosity class share the same kinematical properties. Stars with high velocities form a separate kinematic group, loosely connected to the galactic rotation of the disk, and should be excluded for the samples. In most papers similar to this work, stars with velocity larger than 65 km s^{-1} were discarded. The solution adopted here is more progressive and was obtained by successive iterations of the model to identify the real outliers from the tail of the statistical distribution. Basically from the residuals it was possible to adjust the weighting, that is to say the true magnitude of the random terms ϵ_l and ϵ_b, so that the unit weight variance was close to unity and then to discard the high-velocity stars measured by the magnitude of the residuals properly weighted.

Table 1 sums up the main features of each sample defined by the above selection criteria. The number of selected stars in each group appears in the third column while the percentage of stars of low galactic latitude is given in the following column. As expected most of the young stars which have no yet enough time to leave the spiral arms are found predominantly in the galactic plane. As we sample over older stars the percentage of stars with $|b| < 30°$ decreases to about 0.35-0.4, somewhat below the expected value for an isotropic distribution. The meaning of the last two columns, related to the velocity dispersion, will be explained later in relation with the weighting. The groups are unevenly populated, but none is depleted.

The parallax distribution for each category, is shown in Figs. 5-6 for the parallaxes between 0.5 to 10 mas, with the abscissa referring to the beginning of a class. The vertical axis is given in percentage of the population within each class. The main feature visible in these plots is the progressive change of the average parallax with the spectral type: the early type dwarfs are on the average farther away than the intermediate type, while the the giants K are closer to the Sun than the M giants. This reflects partly the true stellar population in the Galaxy and also a selection effect due to the content of the Hipparcos Catalogue which contains a small population of stars fainter than $V = 10.5$. The intermediate spectral types F5 to K0 have been excluded as they would have given mixed populations of dwarfs and giants, with heterogeneous kinematical properties.

One sees also, that as far as the parallaxes are concerned, the populations from A0 to F0, which are predominantly main sequence stars are nicely distributed to determine the effect of the galactic rotation and the solar motion. The intermediate class F0-F5 should not be trusted too much for the galactic rotation for the lack of distant stars. The last three classes from K0 to M5 comprise mostly old and kinematically evolved red giants and provide a very good material to analyse the velocity dispersion and the galactic rotation.

5.2. Weighting

As mentioned earlier, the real random error required to weight the observation equations is not scaled by the variance of the observed $\mu_l \cos b$ and μ_b, but by that of ϵ_l and ϵ_b, which depends on the velocity dispersion within each stellar group. Let v_{scat} be some measure of the dispersion velocity of a particular group of stars, averaged over all directions. This velocity produces a scatter in the proper motion

$$\mu_{\text{scat}} \approx \frac{v_{\text{scat}}\,\pi}{k}$$

which is function of the distance. At a typical distance of 500 pc and for a dispersion velocity of 15 km s^{-1}, this gives $\mu_{\text{scat}} \sim$ 6 mas, much larger than the random error of the Hipparcos proper motions. Therefore the residual velocities of the stars is the major source of noise in the observation equations and this must be taken care of in the weighting of the equations.

Assuming an equal consequence of v_{scat} on the dispersion on each component of the proper motion (this will be discussed in Sect. 6.4, see also Feast & Whitelock, 1997, Sect. 4), the weighting of the equations should be:

$$W_l = \frac{1}{\sigma_{\mu_l}^2 + \mu_{\text{scat}}^2} \tag{35}$$

$$W_b = \frac{1}{\sigma_{\mu_b}^2 + \mu_{\text{scat}}^2} \tag{36}$$

respectively for the observation equations in proper motion in longitude and latitude. In general the Hipparcos term is negligible compared to the term following from the dispersion velocity. Let $\mathcal{R}_l$ and $\mathcal{R}_b$ be the residuals of the least square fitting in each direction. The unit weight variance,

$$\text{UWV} = \sum_{k=1}^{n_*} \left(W_l \mathcal{R}_l^2 + W_b \mathcal{R}_b^2\right)_k \tag{37}$$

should be close to unity provided the weighting of the equations is properly scaled. Using successive iterations it was possible to determine for each stellar group the value of V_{scat} that ensures that the UWV is close to unity. The values finally used for V_{scat} are given in Table 1 and range from 10 km s^{-1} for early type main sequence stars to 20 km s^{-1} for K and M giants. Using these values to compute the typical random scatter of the proper motion, it is then possible to filter out the outliers by discarding all high-velocity stars with a tangential speed larger than $V_{\text{max}} = 25 + 3\,V_{\text{scat}}$. The constant 25 km s^{-1} accounts for the

Table 2. Components of the Sun motion with respect to different stellar groups. Solution based on the sets of stars listed in Table 1

	Sun velocity and speed (km s^{-1})				Apex(°)	
	$u_\odot$	$v_\odot$	$w_\odot$	$V_\odot$	l_a	b_a
A0 - A5	9.92 ± 0.25	10.71 ± 0.26	6.96 ± 0.21	16.17	47.2	25.5
A5 - F0	11.58 ± 0.32	10.37 ± 0.33	7.19 ± 0.31	17.12	41.8	24.8
F0 - F5	11.46 ± 0.37	11.16 ± 0.37	7.02 ± 0.41	17.47	44.2	23.7
K0 - K5	7.99 ± 0.35	14.97 ± 0.36	7.39 ± 0.40	18.51	61.9	23.5
K5 - M0	8.72 ± 0.49	19.71 ± 0.51	7.28 ± 0.55	22.75	66.1	18.7
M0 - M5	7.37 ± 0.61	20.29 ± 0.63	6.85 ± 0.66	22.65	70.0	17.6

Table 3. Components of the Sun motion with respect to different stellar groups for stars with $|b| < 30°$.

	Sun velocity and speed (km s^{-1})				Apex(°)	
	$u_\odot$	$v_\odot$	$w_\odot$	$V_\odot$	l_a	b_a
A0 - A5	10.37 ± 0.28	11.50 ± 0.29	7.03 ± 0.22	17.01	48.0	24.4
A5 - F0	11.36 ± 0.41	10.30 ± 0.43	7.36 ± 0.32	17.01	42.2	25.7
F0 - F5	11.35 ± 0.61	10.80 ± 0.62	7.30 ± 0.48	17.28	43.6	25.0
K0 - K5	9.88 ± 0.58	14.19 ± 0.64	7.76 ± 0.47	18.95	55.2	24.2
K5 - M0	8.63 ± 0.80	17.43 ± 0.86	7.18 ± 0.64	20.73	63.6	20.3
M0 - M5	8.24 ± 0.92	19.14 ± 0.99	7.54 ± 0.74	22.16	66.7	19.9

asymmetry of the distribution due to the solar motion and the galactic rotation. This threshold is given in the last column of Table 1, and is less than 65 km s^{-1} for early type stars and close to 90 km s^{-1} for K and M giants.

6. Results and discussion

For each run on data summarised in Table 1 we have obtained the components of the solar motion with respect to various stellar groups, the generalized Oort constants presented in Sect. 3 and the values of the dispersion velocity on the three directions of the triad of the galactic coordinates.

6.1. Results for the solar motion

The components of the solar motion are given in Table 2 for all the stars in the specified spectral range and, in Table 3, for a subset limited to galactic latitude less than thirty degrees in absolute value. Columns 2–4 give the components of $\mathbf{v}_\odot$ on the rectangular axes of the galactic frame; the speed and the direction of the apex in galactic longitude and latitude are given in the last three columns.

One must first notice that, as expected, there is no big difference between the solutions restricted to stars lying in the galactic plane and all the stars up to a distance of 2 kpc. This is true for the hot and young stars which are found predominantly at low galactic latitude (Table 1) as well for the later population found also at higher latitude. The component $w_\odot$ for the displacement towards the North Galactic Pole, is fairly constant with the spectral type and has a weighted average of $\bar{w}_\odot = 7.1 \pm 0.2$ km s^{-1} indicating that the Sun is moving upwards from the galactic plane, a result consistent with recent determinations by Comeròn et al., 1994 on stars from O to A0

or Yuan, 1983 for early and late type dwarfs. The agreement is also satisfactory for the two other components. In their recent studies with the Hipparcos cepheids Feast & Whitelock (1997) find 7.6 ± 0.6 km s^{-1} equally consistent with our value for the K-giants. Dehnen & Binney (1998) have restricted their investigation to early and late type dwarfs at moderate distance, precluding the determination of the galactic rotation. Using Oort constants from Feast & Whitelock (1997) they find also a constant upwards velocity with the stellar types with $w_\odot = 7.17 \pm 0.38$ km s^{-1}. The radial component $u_\odot$ is much more variable with a sharp transition between the velocity found with young disk objects with $u_\odot \sim 10 - 11$ km s^{-1} and later types with $u_\odot \sim 7 - 8$ km s^{-1}. Most of the variations is found in the orthoradial component in the galactic plane with $v_\odot$ varying between 10 to 20 km s^{-1} with again two main groups: young stars exhibit an average $v_\odot$ component of the order of 10 to 12 km s^{-1} and late type, comprising mainly giants stars, moving much faster with respect to the Sun with $v_\odot \sim 15 - 18$ km s^{-1}, a result not fundamentally new but well ascertained here on high quality data.

A compilation of many different solutions based on all spectral types and classes is given in Delhaye, 1965 and Mihalas & Biney, 1981 and confirms the large variability of the $v_\odot$ component with the sample (see Dehnen & Binney, 1998 for a thorough discussion on the meaning and interpretation of this variation and its relation with the velocity dispersion). From the APM proper motion project, Evans, 1995 found for the three components of the solar motion measured with red stars (7.3, 13.9, 8.8) km s^{-1}, with an uncertainty of 2 km s^{-1}. The present determination is well within the expected error but has a much better formal accuracy of about 0.2 to 0.5 km s^{-1}, depending mainly on the sample size. A work by Dubath et al., 1988 based only on the radial velocities of late type supergiants has yielded

Table 4. The generalized Oort Constants and their uncertainties determined for the different samples. The angles are in degrees and the amplitudes in $\mathrm{km\,s^{-1}kpc^{-1}}$.

	$\bar{A}$	ϕ	B	$\left[\dfrac{B}{B-A}\right]^{1/2}$	K	A'	ψ	B'	χ
		°					°		°
A0 - A5	11.5 ± 0.8	9.6 ± 2.1	-13.3 ± 0.6	0.733	-0.9 ± 2.4	5.3 ± 1.2	106. ± 13.	3.1 ± 1.2	49. ± 23.
A5 - F0	14.3 ± 1.3	0.2 ± 2.8	-13.2 ± 1.0	0.693	2.7 ± 3.3	5.5 ± 1.6	-43. ± 17.	5.7 ± 1.6	-124. ± 16.
F0 - F5	18.9 ± 2.0	4.9 ± 3.0	-13.0 ± 1.5	0.638	-1.6 ± 4.3	9.6 ± 2.0	-50. ± 12.	9.6 ± 2.0	-119. ± 12.
K0 - K5	13.4 ± 1.9	9.2 ± 4.0	-10.9 ± 1.5	0.669	-0.2 ± 3.0	2.0 ± 1.7	112. ± 47.	2.9 ± 1.7	40. ± 34.
K5 - M0	16.4 ± 2.1	13.9 ± 3.6	-12.4 ± 1.7	0.656	-3.1 ± 3.2	4.1 ± 1.9	-24. ± 28.	1.3 ± 2.0	-23. ± 87.
M0 - M5	14.1 ± 2.0	16.4 ± 4.0	-10.9 ± 1.6	0.660	-4.1 ± 3.1	1.8 ± 1.9	102. ± 59.	1.5 ± 1.9	-26. ± 74.

Table 5. The generalized Oort Constants and their uncertainties determined for the different samples and for $|b| < 30°$. The angles are in degrees and the amplitudes in $\mathrm{km\,s^{-1}kpc^{-1}}$.

	$\bar{A}$	ϕ	B	$\left[\dfrac{B}{B-A}\right]^{1/2}$	K	A'	ψ	B'	χ
		°					°		°
A0 - A5	10.9 ± 0.8	7.6 ± 2.2	-13.3 ± 0.6	0.741	-0.5 ± 3.0	1.9 ± 2.0	142. ± 61.	2.6 ± 2.0	-25. ± 44.
A5 - F0	14.0 ± 1.3	0.1 ± 2.8	-13.3 ± 1.0	0.699	-1.1 ± 4.6	14.6 ± 3.1	-66. ± 12.	13.8 ± 3.1	-111. ± 13.
F0 - F5	19.4 ± 2.1	1.6 ± 3.0	-12.1 ± 1.5	0.620	4.0 ± 7.8	23.2 ± 5.2	-69. ± 13.	23.0 ± 5.2	-111. ± 13.
K0 - K5	12.5 ± 2.3	15.2 ± 5.3	-10.9 ± 1.7	0.682	-8.2 ± 6.6	1.4 ± 4.4	-77. ± 190.	3.7 ± 4.4	-56. ± 69.
K5 - M0	20.6 ± 2.7	16.1 ± 3.7	-11.0 ± 2.0	0.590	-9.1 ± 7.1	1.9 ± 5.2	166. ± 143.	5.1 ± 4.8	0. ± 53.
M0 - M5	14.6 ± 2.5	14.9 ± 4.8	-11.7 ± 1.9	0.667	-4.5 ± 6.0	8.9 ± 4.4	52. ± 29.	6.3 ± 4.3	140. ± 39.

Table 6. Velocity dispersion parameters in the galactic frame for various type of star, with $r_1 = \langle v^2 \rangle^{1/2} / \langle u^2 \rangle^{1/2}$, $r_2 = \langle w^2 \rangle^{1/2} / \langle u^2 \rangle^{1/2}$.

	Dispersions (km s^{-1})				
	$\langle u^2 \rangle^{1/2}$	$\langle v^2 \rangle^{1/2}$	$\langle w^2 \rangle^{1/2}$	r_1	r_2
A0 - A5	17.03 ± 0.21	11.26 ± 0.34	7.16 ± 0.36	0.66	0.42
A5 - F0	19.81 ± 0.25	13.39 ± 0.39	8.07 ± 0.51	0.68	0.41
F0 - F5	22.54 ± 0.28	15.29 ± 0.43	9.94 ± 0.66	0.68	0.44
K0 - K5	30.45 ± 0.27	20.51 ± 0.42	16.04 ± 0.54	0.67	0.53
K5 - M0	30.99 ± 0.39	22.44 ± 0.56	17.21 ± 0.71	0.72	0.56
M0 - M5	32.21 ± 0.47	23.11 ± 0.70	18.30 ± 0.81	0.72	0.57

$u_\odot = 9.7 \pm 1.3$ km s^{-1} and $v_\odot = 13.0 \pm 1.1$ km s^{-1}, significantly smaller than the determination of this paper for the K0 - K5 sample. But our sample comprises mainly ordinary giants rather than supergiants, which is sufficient to account for the difference (see also Mihalas & Biney, 1981). (There is no information from the radial velocity on $w_\odot$ for stars lying primarily in the galactic plane.) Finally the result in Table 2 and 3 for A stars agrees closely with the basic solar motion $(9, 11, 6)$ km s^{-1} defined by Mihalas & Biney, 1981 with A and K stars in the solar neighborhood.

6.2. The Oort constants

6.2.1. The constant A

The values derived for the generalized Oort constants, $\bar{A}, B, K, A', B'$, are given with their formal uncertainties in

Table 4 for all the stars and in Table 5 for objects with galactic latitude less than thirty degrees. Recall that the IAU values are $A = 15$ km s^{-1}kpc^{-1} and $B = -10$ km s^{-1}kpc^{-1}, consistent with the adoption of $R_\odot = 10$ kpc and the rotation velocity at the distance $R_\odot$, $\Theta_\odot = 250$ km s^{-1}. These values can be regarded as conventional with no pretense today of being the truth. A weighted average of various measurements given by Mihalas & Biney, 1981 is $A = 16 \pm 2$ km s^{-1}kpc^{-1} and $B = -11.1 \pm 3$ km s^{-1}kpc^{-1} while at the same time he pointed out that these values should be regarded as provisional because the data upon which they rest are not yet of sufficient quality to yield definite values.

In Tables 4 - 5 we have also given the combination

$$\left[\frac{B}{B-A}\right]^{1/2} \tag{38}$$

as being particularly relevant for the epicyclic motion in the galactic plane and the velocity dispersion (see Sect. 6.3 and Table 6) and in addition should be more constant with the spectral type than the generalised Oort constants. From dynamical considerations, one expects this ratio to be of the order of 0.62 for kinematically evolved stellar groups.

The parameter $\bar{A}$ fluctuates significantly outside the formal error bars from one category to another. A straight mean yields $A \approx 14.7 \pm 1.0$ km s^{-1}kpc^{-1} when all galactic latitudes are considered and $A \approx 15.2 \pm 1.5$ km s^{-1}kpc^{-1} when $|b| < 30°$. However the more distant stars are better suited to build up the systematic effect of the galactic rotation on the proper motion and, in this respect, the classes A0 - A5 and the giants have more weight than the A5 to F5 (see Figs. 5-6). From that, it is difficult

not to accept a systematic difference between the young stars lying in the disk, with A close to 11 km s^{-1}kpc^{-1} and the giant stars with a value larger of 14.5 km s^{-1}kpc^{-1} each with an uncertainty of 1 km s^{-1}kpc^{-1}.

Compared to recent determinations reviewed by Kerr & Lynden-Bell, 1986 the latter value is comparable to the various measurements quoted in this paper which average to 14.4 ± 0.7 km s^{-1}kpc^{-1}. The recent work of Miyamoto & Sôma, 1993a based on 30 000 K–M giants from the 185 000 stars of the Astrographic Catalogue of Reference Stars, very similar in spirit to this investigation, ends up with $A \sim 12 - 13 \pm 0.6$ km s^{-1}kpc^{-1} according to the constraints set in the various runs. At the other extreme, Comeròn et al., 1994 have considered samples of O and B stars from the Hipparcos Input Catalogue and derived a low value of A in the range 10 to 11.3 km s^{-1}kpc^{-1} with an uncertainty close to 1 km s^{-1}kpc^{-1}. This also in agreement with Hanson, 1987 who obtains $A = 11.3 \pm 1.06$ km s^{-1}kpc^{-1} from the faint stars of the Lick Northern Proper Motion program. However in their study of radial velocities of 272 supergiants at distance as large as 3 kpc, Dubath et al., 1988 have obtained $A = 16 \pm 1.5$ km s^{-1}kpc^{-1} and even a larger value when the investigation is restricted to local distances $d \sim 1 - 1.5$ kpc. This high value was also obtained from the proper motions of the FK4 stars by Fricke & Tsioumis, 1975 with $A = 15.6 \pm 0.7$ km s^{-1}kpc^{-1}, but with a very small sample of heterogeneous objects. The most recent investigation from a well selected set of Cepheids by Feast & Whitelock (1997) ended up with $A = 14.8 \pm 0.9$ km s^{-1}kpc^{-1}, quite similar to the present solution for the giants. Because these Cepheids are rather faint, only a very small fraction of the sample studied by Feast and Whitelock appears in our selection of giant stars.

6.2.2. The constant B

Let us consider now the constant B whose value can only be derived from the stellar proper motions, provided that the inertiality of the frame to which these motions are referred is well ascertained in order to limit the systematic errors and make the interpretation of the result relatively straightforward. This is the case with the Hipparcos proper motions which are completely independent on the precessional constants unlike that of the FK5 and of all other derived stellar catalogues in the visible. As stated in the introduction of this paper, the present determination of B should not be hampered by the coupling between the galactic vorticity and the residual rotation left in the reference frame.

Looking at the individual results in Tables 4 - 5 one does not see significant difference between the runs carried out with all the stars or with the restriction to the vicinity of the galactic plane. There is again a variation with spectral types and classes but hardly significant with this data, with $B = -13.2 \pm 0.5$ km s^{-1}kpc^{-1} for early types dwarfs and $B = -11.5 \pm 1$ km s^{-1}kpc^{-1} for distant giants.

The review of Kerr & Lynden-Bell, 1986 gives $B = -12.0 \pm 0.7$ km s^{-1}kpc^{-1}. In his work on the Lick Proper Mo-

tion, Hanson, 1987 obtains $B = -13.91 \pm 0.92$ km s^{-1}kpc^{-1} for a fit over 60 000 faint stars (16th magnitude) with absolute proper motions measured with respect to an extragalactic frame. Owing to the large number of stars, he investigated the galactic rotation per zone of galactic latitude and found no significant change in the Oort constants with galactic latitude. In their work with the Hipparcos Cepheids Feast & Whitelock (1997) find $B = -12.3 \pm 0.6$ km s^{-1}kpc^{-1} again compatible with the above results in particular with the solution for the K-giants.

The investigation of Miyamoto & Sôma, 1993a on K–M giants leads to $B = -8.5 \pm 0.6$ km s^{-1}kpc^{-1}, in disagreement with the above results for late type giants. On the other hand Comeròn et al., 1994 with 1151 stars B6 - A0, have obtained $B = -13.2 \pm 1.4$ km s^{-1}kpc^{-1}. This and the present work tend to support the idea that there is a systematic difference in the global differential velocity field between the early type dwarfs and late type giants, which are known anyhow to belong to separate kinematics groups.

Our determination of B refers to the Hipparcos system of proper motions, which may have a systematic rotation relative to the extragalactic system. As stated in Sect. 2, the link has an overall uncertainty of 0.25 mas/yr or 1.2 km s^{-1}kpc^{-1} which should be added to the formal error of the least squares fitting for B and in fact dominates the latter. The formal error represents the uncertainty in the vorticity in the Hipparcos frame while the combined uncertainty is a measure of our knowledge of the absolute vorticity. The same remark applies in the determination of ω_r and ω_θ below.

6.2.3. Combinations of Oort constants

There are two relevant combinations of A and B: The difference $A - B = \Theta/R_\odot = \Omega(R_\odot)$ and the ratio of Eq. (38). Averaging between the dwarfs and the giants one finds $A - B = 25.1 \pm 0.8$ km s^{-1}kpc^{-1} which gives with using $R_\odot = 8.5 \pm 0.2$ kpc (Kerr & Lynden-Bell, 1986, Feast & Whitelock, 1997) the rotational speed $\Theta_\odot = 213 \pm 7$ km s^{-1}, a value much smaller than the IAU value of 250 km s^{-1}, compatible with the 222 km s^{-1} given by Kerr & Lynden-Bell, 1986 or with the value derived by Mihalas & Biney, 1981 with $\Theta_\odot = 245 \pm 40$ km s^{-1}. The determination of $\Omega(R_\odot)$ averaged over different categories of stars comes very close to the Feast and Whitelock value $\Omega(R_\odot) = 27.2 \pm 0.9$ km s^{-1}kpc^{-1}) from the Hipparcos Cepheids.

Regarding the ratio of Eq. (38), the individual values appear in Tables 4 - 5 and show a good consistency. Because this ratio is linked to the velocity dispersion, it is particularly meaningful for evolved stars like the K - M giants and to a lesser extent the F - G dwarfs, while it should not be considered for the earlier types. This point will be discussed in the next section. For these three classes, the value is remarkably well defined at 0.662 ± 0.004. One must note that despite marked variations in the individual values of A and B between the two sets of runs, the velocity-ellipsoid ratios are very similar for the corresponding spectral classes with or without limitations in galactic latitude and when it is expected to be well defined, it is found constant within the different classes. This gives a certain confidence that the

procedures followed in this study is not grossly flawed and the set of values is meaningful for the Milky Way.

The remaining parameters in Tables 4 - 5 are not determined with the same level of significance and only the phases ϕ in the third column deserve attention. The phase is definitely positive with the straight average $6.2 \pm 1.5\,^\circ$ which gives $C = \bar{A}\sin 2\phi \sim 2.5 \pm 0.6$ km s^{-1}kpc^{-1} very close to a preliminary determination based on the harmonic analysis of the Hipparcos proper motions carried out by Mignard & Frœschlé, 1996.

Going back to the definition of C in term of the derivatives of the velocity field with Eqs. (8, 19-22), this means that the components S_{rr} and $S_{\theta\theta}$ are non-zero. This is connected to the orientation of the $x-$axis of the galactic coordinate system in Fig. 2 which is directed toward the galactic centre, while in fact there is no physical connection which guarantees that this is in fact the case. Eqs. (21 - 22) show that by shifting the origin of the galactic longitude by ϕ would make $C \equiv 0$, or $S_{rr} = S_{\theta\theta} = 0$. This can be stated in a slightly different way by considering the change of the components of the tensor **S** under a rotation of angle ϕ about the $z-$axis. If initially we have $S_{rr} = S_{\theta\theta} = 0$ and $S_{r\theta} \neq 0$, we have in the new frame

$$\tilde{S}_{r\theta} = S_{r\theta}\cos 2\phi \tag{39}$$

$$\tilde{S}_{rr} = S_{r\theta}\sin 2\phi \tag{40}$$

$$\tilde{S}_{\theta\theta} = -S_{r\theta}\sin 2\phi \tag{41}$$

which provides another hint on the meaning of the phase offset and casts light on the C term.

The galactic frame was defined by a conventional transformation from the equatorial system, the inertial frame to which the Hipparcos Catalogue is referred, by the coordinates of the galactic pole and the longitude in the galactic plane of a fiducial origin for the galactic longitude. It is then not very surprising that this purely geometric definition of the direction of the galactic centre, does not provide the perfect centre of symmetry with respect to which the description of the galactic rotation would look simple. By shifting the fiducial centre by about 6 degrees, the local velocity field would appear more symmetric with no radial term ($V_r = 0$) and no azimuthal dependance of the rotation speed ($\partial V_\theta / \partial \theta = 0$). In other words, with the adopted galactic frame, the rotation speed of the LSR is not perpendicular to the direction of the Galactic centre but tilted by about 6 degrees and the velocity field would appear more symmetric with respect to the axes of the tilted frame.

The K term is also linked to the components S_{rr}, $S_{\theta\theta}$ of **S** and more generally to $\nabla \cdot \mathbf{V}$. However the derived values are far too uncertain to lead to a valuable interpretation for a subject as tricky as the local expansion or contraction. In addition, as mentioned earlier without radial velocity one derivative (e.g S_{zz}) remains unknown. The same conclusion is valid for A' and B' and their phases. What matters are in fact the terms $A'\cos\psi$, $A'\sin\psi$ and similarly $B'\cos\chi$, $B'\sin\chi$, which show nothing systematic with the spectral type, as can be seen just from the scatter of the phases. As B' is related to ω_r and ω_θ this implies that the only rotation component really significant is perpendicular to the galactic plane, in contradic-

tion with the claim by Miyamoto & Sôma, 1993b of a kinematic galactic wrap for the O - B stars.

As a conclusion of this section on the parameters of the model, it can be said that in spite of the quality of the Hipparcos proper motions, it is not possible with data limited in distance to 2 pc to go much further than the Oort-Lindblad model of an axisymmetric and plane parallel rotating Galaxy. One must even say that this is already an extrapolation from the differential flow determined with only two non-zero components of the velocity strain tensor. In order to test the robustness of the solutions to these non-significant terms in the model, several runs were computed by constraining all the coefficients S_{kl} and ω_k to be zero but $S_{r\theta} = A$, $\omega_z = B$. No significant changes were observed in the results, which was in fact expected as a result of the virtual absence of correlation between the various parameters, except between S_{rr} and $S_{\theta\theta}$ with $\rho = 0.85$. But only their sum and difference are physically interesting and are not correlated. In addition when only small galactic latitudes are sampled, there is a non negligible correlation (~ 0.7) between $S_{\theta z}$, ω_r and S_{rz}, ω_θ as is easily understood from the design matrix when $\cos b \sim 1$.

A provisional conclusion of this section would be that given the high quality of the proper motions available, the fact that the remaining uncertainty of the inertiality of the reference frame is much smaller than the scatter of the parameters A, B with the star sample, this is the very concept of Oort's constant that should be questioned and thus that of the description of the overall motion with the superposition of continuous flows.

7. The velocity dispersion

The examination of the residuals after the fit, provides interesting clues as to the statistical distribution of the components of the peculiar velocity of the stars. The peculiar velocity is assumed to follow a three dimensional gaussian distribution (Schwarzschild, 1907) with uncorrelated components u, v, w on the triad **i**, **j**, **k**. With the exception of the very early type stars, this is known to be true, since the vertex of the dispersion ellipsoid is within 10 to 20 degrees of the galactic center.

Hence, the distribution function is proportional to,

$$\frac{1}{8\pi^3 \langle u^2\rangle \langle v^2\rangle \langle w^2\rangle} \times$$
$$\exp\left[-\frac{u^2}{2\langle u^2\rangle} - \frac{v^2}{2\langle v^2\rangle} - \frac{w^2}{2\langle w^2\rangle}\right] \tag{42}$$

and the peculiar velocity $\mathbf{v} : (u, v, w)$ of a star may be considered as a random vector whose probability function is given by Eq. (42). An observation in the direction of galactic coordinates l, b is tied to the random velocity vector expressed on the local triad $\boldsymbol{e}_r$, $\boldsymbol{e}_l$, $\boldsymbol{e}_b$ attached to the spherical coordinates l, b of the star at M by Eqs. 11. If the proper motion components and the radial velocity were available one could solve Eqs. 11 for $v_x = u$, $v_y = v$ $v_z = w$ for all the residuals and study directly the dispersions $\langle u^2\rangle$, $\langle v^2\rangle$, $\langle w^2\rangle$ from the moments of the empirical distributions. With the limited information carried

by the proper motion one only has the following two relations between random variables,

$$v_l = \frac{k\,\mu_l\,\cos b}{\pi} = -u\,\sin l + v\,\cos l$$
$$v_b = \frac{k\,\mu_b}{\pi} = -u\,\sin b\cos l - v\,\sin b\sin l + w\,\cos b \qquad (43)$$

We have then with E[.] for the mathematical expectation,

$$E[v_l^2] = \langle u^2 \rangle \sin^2 l + \langle v^2 \rangle \cos^2 l \qquad (44)$$
$$E[v_b^2] = \langle u^2 \rangle \sin^2 b \cos^2 l + \langle v^2 \rangle \sin^2 b \sin^2 l$$
$$+ \langle w^2 \rangle \cos^2 b \qquad (45)$$

which can be solved by least squares for the components of the velocity dispersion with the residuals of the least squares fitting after the galactic rotation and the solar motion have been removed from the proper motion signal. From the formal error $\sigma_{\langle u^2 \rangle}, \cdots$ one obtains

$$\sigma_{\langle u^2 \rangle^{1/2}} = \frac{\sigma_{\langle u^2 \rangle}}{2\,\langle u^2 \rangle^{1/2}} \qquad (46)$$

Results appear in Table 6 for the same sampling as before. For all types we have the classical result that the dispersion is larger in the radial direction than in the orthoradial and that the latter is systematically larger than the dispersion perpendicular to the galactic plane. We have thus computed the ratios

$$r_1 = \langle v^2 \rangle^{1/2} / \langle u^2 \rangle^{1/2}$$

and

$$r_2 = \langle w^2 \rangle^{1/2} / \langle u^2 \rangle^{1/2}\,.$$

and found that, except for very young stars, r_1 and r_2 are fairly constant with $r_1 \approx 0.65$ to 0.75 and more important for the dynamics of the Galaxy $r_2 \approx 0.45$ to 0.55. r_1 is also related to the Oort constants through the expression established for example in Binney & Tremaine, 1987 from the epicyclic theory,

$$r_1^2 = \frac{\langle v^2 \rangle}{\langle u^2 \rangle} = \frac{B}{B - A}. \qquad (47)$$

Various determinations have led to the conclusion that this ratio is close to 0.40, or 0.63 for its square root (Kerr & Lynden-Bell, 1986). This ratio in terms of the Oort constants is discussed in the previous section and the determination is given in Tables 4- 5. There is a significant difference between the ratio of the velocity dispersion, close to 0.72 for the dynamically relaxed red giants, and the ratio computed with the Oort constants A, and B which is of the order of 0.66. It is troublesome that the agreement is better for the main sequence stars, except the very early types, which are not supposed to be in a steady dynamical state and for which one would not be surprised to find a difference between the two approaches. A discussion by Gilmore et al., 1989 indicates also a variation with the metallicity of the stars with r_1 between 0.59 to 0.78 which deserves more attention. With their well selected sample of 12 000 main sequence stars Dehnen & Binney (1998) arrive at $r_1 = 0.63$

and $r_2 = 0.45$ with a trend similar, but more conspicuous, to that found in this paper with the increasing star colour.

As already mentioned in relation to the unit weight variance, the dispersion is much smaller for the early type stars of the disks than for the older objects of spectral type later than G, although the transition is very gradual. This fact has been known for long, and results for the repeated close approaches that lead to a progressive growth of the dispersion as the number of interactions with stars or molecular clouds becomes larger with time. Younger stars are observed where they formed and retain the kinematical properties of the interstellar medium from which they originated. Older objects have started to relax and are close to the equilibrium for their radial and vertical (perpendicular to the galactic plane) motions.

There is an interesting relationship between the components of the velocity dispersion and the random scatter introduced in Sect. 5.2 for the weighting with $v_{\rm scat}$. In Table 1 the scatter was determined by constraining the unit weight variance to be close to unity. As this was ultimately based on the average magnitude of the residuals, this is closely related to the velocity dispersion. From Eqs. (45) one finds with $\langle \cos^2 l \rangle = \langle \sin^2 l \rangle = 1/2$,

$$E[v_l^2] = \frac{1}{2}\,(1 + r_1^2)\,\langle u^2 \rangle \qquad (48)$$

$$E[v_b^2] = \left[\frac{1}{2}\,\langle \sin^2 b \rangle\,(1 + r_1^2) + \langle \cos^2 b \rangle\,r_2^2 \right] \langle u^2 \rangle \qquad (49)$$

which depends weakly on the distribution of the stars with the galactic latitude. For early type stars orbiting in the galactic disk, $\langle \sin^2 b \rangle \sim 0$ and

$$E[v_b^2] \sim r_2^2\,\langle u^2 \rangle\,.$$

On the opposite, for a uniform distribution on the celestial sphere, $\langle \sin^2 b \rangle = 1/3$ and $\langle \cos^2 b \rangle = 2/3$. So we can state without big error with $r_1 \sim 0.7$ and $r_2 \sim 0.5$ that

$$E[v_l^2] \approx 0.7\,\langle u^2 \rangle$$

and

$$E[v_b^2] \approx 0.25\,\langle u^2 \rangle\,,$$

for stars of low galactic latitude and

$$E[v_b^2] \approx 0.42\,\langle u^2 \rangle\,,$$

when the distribution in galactic latitude is more uniform. Taking the square root and $\langle u^2 \rangle^{1/2}$ from Table 6 one gets for $v_{\rm scat}$ and for each spectral type values comparable to those in Table 1 used for the weighting. To illustrate this point, the scatters in Fig. 8 for the A5 - F0 selection are respectively 15.7 km s^{-1} and 9.9 km s^{-1} in longitude and latitude, while $\sqrt{0.7\,\langle u^2 \rangle} = 16.5$ km s^{-1} and $\sqrt{0.25\,\langle u^2 \rangle} = 9.9$ km s^{-1}. For the red giants with a sample in b more uniform one finds $\sqrt{0.7\,\langle u^2 \rangle} = 25.5$ km s^{-1} and $\sqrt{0.42\,\langle u^2 \rangle} = 19.7$ km s^{-1}, while the observed dispersions in Fig. 8 (robust estimation) are respectively 25.3 km s^{-1} and 19.8 km s^{-1}. Following this argument it would be sensible to weight the observation equations in $\mu_l \cos b$ and μ_b with different weights. Trials on limited cases have shown that this does not change the results presented in the previous sections and this refinement was not implemented.
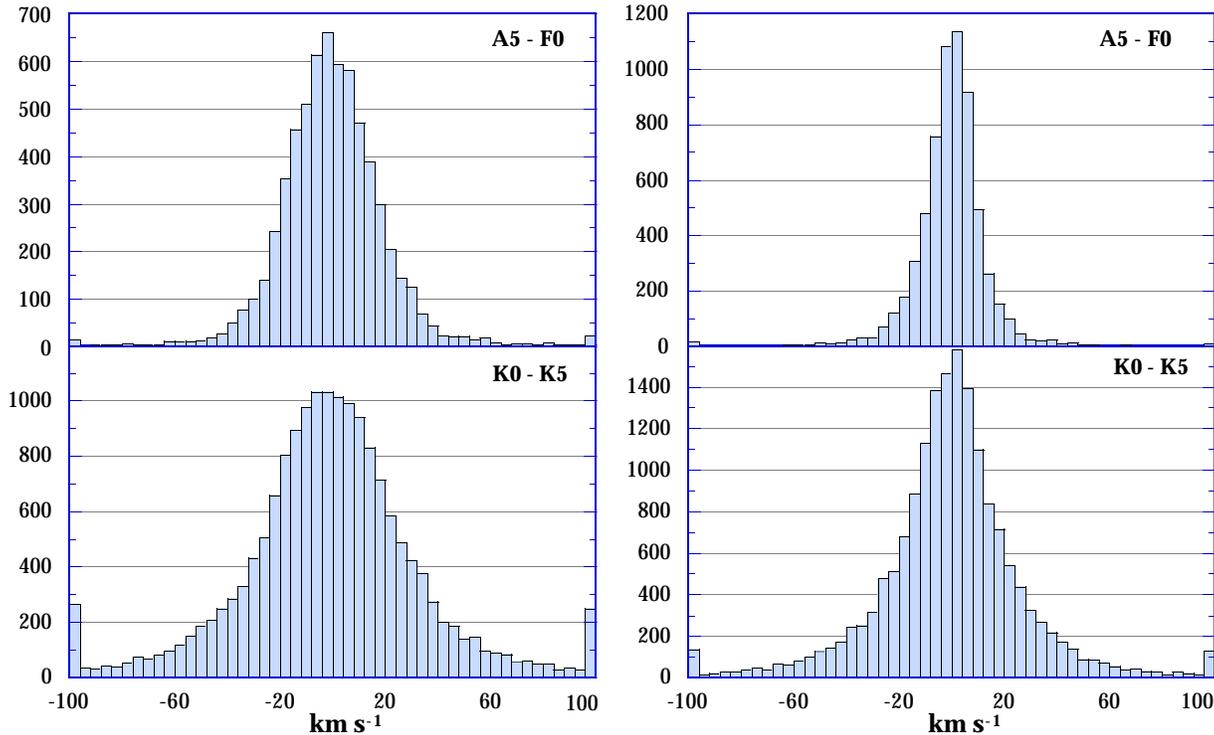
Fig. 8. Distribution of the residuals in velocity in longitude (left) and latitude (right) for a typical run with stars A5 - F0 in the upper panel and K0 - K5 in the lower panel. The run has been done by downweighting the high-velocity stars, so that they do not enter the least-squares fitting, but can be included in the residuals. As expected from the anisotropy of the velocity distribution, the dispersion is less pronounced in latitude than in longitude. The population of rejected stars appear in the tails. Stars with velocities larger than 70 km s^{-1} (A5 - F0) or 88 km s^{-1} (K0 - K5) are not included in the least squares fit.

8. Conclusion

The quality and homogeneity of the Hipparcos proper motions and parallaxes have allowed to investigate globally the velocity field of the stars in the solar neighborhood within 2 kpc as a function of the spectral type and for various zones of galactic latitude. For each group the magnitude cutoff was determined from the completeness of the sample to avoid statistical bias. The velocity field has been modeled with a superposition of three independent kinematical factors:

1. The reflex motion due to the sun peculiar velocity
2. The differential velocity field induced by the galactic rotation
3. The random effect of the peculiar velocity of the individual stars

The observational effects on the proper motions have been parameterized in galactic coordinates and investigated for each spectral types and for dwarfs and ordinary giants. The value of the solar motion relative to the Local Standard of Rest has been determined together with the set of generalised Oort constants. Although the galactic model was more general than the usual plane parallel axisymmetric rotation, the results show that the Oort-Lindblad model, with a significant shift of the symmetry axis from the galactic centre, is sufficient to describe the galactic global motion in the vicinity of the solar system, at least with the accuracy permitted with the Hipparcos proper motions and

parallaxes. The axes of the velocity ellipsoid for most spectral types are assessed with an accuracy of 0.2 to 0.5 km s^{-1}.

However the scatter of the results with the stellar sample, larger than what can be expected from the uncertainty in the data, calls strongly for a reexamination of the concept of laminar flow to describe the overall galactic rotation. This becomes all the more important because of the prospect of a much larger kinematical mapping of the Galaxy with the approved or planned astrometry mission like FAME or GAIA.

References

Arenou F., Lindegren L., Frœschlé M., et al., 1995, A&A 304, 52
Binney J., Tremaine S., 1987, Galactic Dynamics. Chap. 3–4, Princeton Series in Astrophysics
Clube S.V.M., 1972, MNRAS 159, 289
Comeròn F., Torra J., Gòmez A.E., 1994, A&A 286, 789
Crézé M., 1970, A&A 9, 405
Dehnen W., Binney J.J., 1998, MNRAS 298, 387
Delhaye J., 1965, in: Blaauw A., Schmidt M. (eds.), Galactic Structure, Stars and Stellar Systems. vol. 5, Univ. of Chicago Press
Dubath P., Mayor M., Burki G., 1998, A&A 205, 77
ESA, 1997, The Hipparcos and Tycho Catalogues. ESA SP-1200, Vol. 1–4

Evans D.W., Irwin M., 1995, MNRAS 277, 820

Feast M., Whitelock P., 1997, MNRAS 291, 683

Fricke W., Tsioumis A., 1975, A&A 42, 449 Mignard F., Arenou F., 1997, in: Perryman M., Bernacca P.L. (eds.), Hipparcos Venice '97, ESA SP-402, p. 49

Gilmore G., Wyse R.F.G., Kuijken K., 1989, ARA&A 27, 555

Hanson R.B., 1987, AJ 94, 409

Hoskin M., 1982, Stellar Astronomy. Science History Publications

Kerr F.J., Lynden-Bell D., 1986, MNRAS 221, 1023

Kovalevsky J., Lindegren L., 1995, A&A 304, 189

Kovalevsky J., Lindegren L., Perryman M.A.C., 1997, A&A 323, 620

Landau L., Lifchitz E., 1967, Theory of Elasticity

Lindblad B., 1925, Ark. för Mat. Astron. 19A, 21

Love A.E.H., 1944, A treatise on the mathematical theory of elasticity. Dover

Mignard F., Frœschlé M., 1996, in: Frœschlé M., Mignard F. (eds.), Proc. of the Deuxième Atelier du Groupe de Recherche en Astronomie Spatiale, Grasse, 26-27 September 1995, p 185

Mignard F., 1997, in: Perryman M., Bernacca P.L. (eds.), Hipparcos Venice '97, ESA SP-402, p.

Mihalas D., Biney J., 1981, Galactic Astronomy. Freeman

Milne E.A., 1936, MNRAS 95, 560

Miyamoto M., Sôma M., 1993a, AJ 105, 691

Miyamoto M., Sôma M., Yoshizawa M., 1993b, AJ 105, 2138

North J.D., 1990, The Measure of the Universe. Dover Publications

Ogorodnikov K.F., 1932, Z. Astrophys. 4, 190

Ogorodnikov K.F., 1965, Dynamics of stellar systems. Pergamon Press

Oort J.H., 1927a, Bull. Astron. Inst. Neth. 3, 275

Oort J.H., 1927b, Bull. Astron. Inst. Neth. 4, 79

Perryman M.A.C., Lindegren L., Kovalevsky J., et al., 1997, A&A 323, L49

Ratnatunga K.A., 1992, Galactic structure, Stellar kinematics in The Astronomy and Astrophysics Encyclopedia. Cambridge University Press

Schwarzschild K., 1907, Göttingen Nachr., 614

Yuan C., 1983, Kinematics, Dynamics and Structure of the Milky Way. D. Reidel Pub. Comp., p. 47